Journal of the American Heart Association

ORIGINAL RESEARCH

# Aging Impairs Mitochondrial Function and Mitophagy and Elevates Interleukin 6 Within the Cerebral Vasculature

Daniel J. Tyrrell, PhD; Muriel G. Blin, PhD; Jianrui Song, PhD; Sherri C. Wood, BS; Daniel R. Goldstein, MD

**BACKGROUND:** The blood-brain barrier (BBB) is critical for cerebrovascular health. Although aging impairs the integrity of the BBB, the mechanisms behind this phenomenon are not clear. As mitochondrial components activate inflammation as mitochondria become dysfunctional, we examined how aging impacts cerebrovascular mitochondrial function, mitophagy, and inflammatory signaling; and whether any alterations correlate with BBB function.

**METHODS AND RESULTS:** We isolated cerebral vessels from young (2–3 months of age) and aged (18–19 months of age) mice and found that aging led to increases in the cyclin-dependent kinase inhibitor 1 senescence marker with impaired mitochondrial function, which correlated with aged mice exhibiting increased BBB leak compared with young mice. Cerebral vessels also exhibited increased expression of mitophagy proteins Parkin and Nix with aging. Using mitophagy reporter (mtKeima) mice, we found that the capacity to increase mitophagy from baseline within the cerebral vessels on rotenone treatment was reduced with aging. Aging within the cerebral vessels also led to the upregulation of the stimulator of interferon genes and increased interleukin 6 (IL-6), a cytokine that alters mitochondrial function. Importantly, exogenous IL-6 treatment of young cerebral vessels upregulated mitophagy and Parkin and impaired mitochondrial function; whereas inhibiting IL-6 in aged cerebral vessels reduced Parkin expression and increased mitochondrial function. Furthermore, treating cerebral vessels of young mice with mitochondrial N-formyl peptides upregulated IL-6, increased Parkin, and reduced Claudin-5, a tight junction protein integral to BBB integrity.

**CONCLUSIONS:** Aging alters the cerebral vasculature to impair mitochondrial function and mitophagy and increase IL-6 levels. These alterations may impair BBB integrity and potentially reduce cerebrovascular health with aging.

**Key Words:** aging ■ cerebrovascular inflammation ■ interleukin 6 ■ mitophagy

Aging disrupts the blood-brain barrier (BBB), which is critical for maintaining healthy cerebrovascular function,[1] via unclear mechanisms. Vascular aging leads to impaired mitochondrial bioenergetics and quality control,[2,3] increased inflammation,[4] increased oxidative stress,[5] senescence,[6] and fibrosis.[7] Of the potential mechanisms by which aging impairs the BBB, the vasculature is an area that has been underappreciated until recently.[8] Vascular aging could also impact the integrity of the BBB by reducing the delivery of critical nutrients, such as oxygen, glucose, and amino acids, to neuronal tissue. Furthermore, vascular aging impairs clearance of carbon dioxide, amyloid-β, and other waste products from the brain.[1] But whether any of these changes occur within the cerebral vasculature with aging to disrupt the BBB is unclear.

The role of mitochondria in contributing to vascular aging and disease has been increasingly recognized, although this has not been specifically examined in the cerebral vasculature. Aortic mitochondrial dysfunction occurs by 18 months of age in mice and in atherosclerotic regions of the aorta in older adults (ie,

Correspondence to: Daniel J. Tyrrell, PhD, or Daniel R. Goldstein, MD, NCRC B020-209W, 2800 Plymouth Rd, Ann Arbor, MI 48104. E-mail: dantyrr@umich.edu (or) drgoldst@umich.edu

Supplementary Material for this article is available at https://www.ahajournals.org/doi/suppl/10.1161/JAHA.120.017820

For Sources of Funding and Disclosures, see page 12.



*JAHA* is available at: www.ahajournals.org/journal/jaha

## CLINICAL PERSPECTIVE

### What Is New?

- Our study reveals that aging impairs mitochondrial function and mitophagy (a process to remove defective mitochondria) within the cerebral vasculature in mice. We correlated these findings to impaired blood-brain barrier integrity with aging.
- Age-associated alterations in mitochondrial function, mitophagy, and blood-brain barrier integrity associate with elevation of the cytokine interleukin 6 within the cerebral vasculature.
- Inhibiting interleukin 6 improves mitochondrial function in the cerebral vasculature of aged mice.

### What Are the Clinical Implications?

- Older people exhibit an increase in mortality and morbidity from stroke and exhibit small-vessel cerebrovascular disease.
- Our study reveals that damaged mitochondria and a reduced ability to remove these damaged mitochondria may contribute to this aged vascular phenotype.
- Therapies that either improve mitochondrial function or increase mitochondrial turnover, potentially by inhibiting interleukin 6, may improve cerebrovascular health with aging.

### Nonstandard Abbreviations and Acronyms

| | |
|---|---|
| **BBB** | blood-brain barrier |
| **FPR1** | formyl peptide receptor 1 |
| **MCA** | middle cerebral artery |
| **mtDAMP** | mitochondrial damage-associated molecular pattern |
| **OCR** | oxygen consumption rate |
| **p21** | cyclin-dependent kinase inhibitor 1 |
| **PGC1-α** | peroxisome proliferator-activated receptor γ coactivator |
| **PINK1** | phosphatase and tensin homolog-induced kinase 1 |
| **STING** | stimulator of interferon genes |
| **WT** | wild type |

>70 years of age).[9-11] Mitochondrial dysfunction leads to mitochondrial components, such as mitochondrial DNA, cardiolipin, and N-formyl peptides, spilling into the cytosol. These components act as mitochondrial damage-associated molecular patterns (mtDAMPs) to induce inflammation by activating either the Toll-like receptor 9,[12] cyclic GMP-AMP synthase, or stimulator of interferon genes (STING) pathways.[13,14] The upregulation of interleukin 6 (IL-6) within the aortas of mice with aging[9] suggests that activation of all of these pathways may occur with vascular aging. Yet, the role of mtDAMPs in promoting inflammation during aging in the cerebral vasculature is unclear. As systemic administration of exogenous N-formyl peptides in rats increases vascular permeability in the aorta,[15] and because cerebrovascular inflammation disrupts BBB function and enhances neuronal death,[16] vascular aging may impair neuronal health by reducing BBB integrity.

One homeostatic mechanism to reduce the inflammatory effects of mtDAMPs is to effectively recycle damaged mitochondria via mitophagy, a specialized subset of macroautophagy.[17] The protein PINK1 (phosphatase and tensin homolog-induced kinase 1), a serine/threonine kinase, accumulates on the outer membrane of damaged mitochondria and recruits Parkin, an E3-ubiquitin ligase,[18-20] which ubiquitinates mitochondrial outer membrane proteins.[21] This primes mitochondria for autophagy machinery, sequestosome 1 (denoted as p62) and Map1LC3b (LC3), to package dysfunctional mitochondria in autophagosomes for degradation in lysosomes.[22] Although basal mitophagy in the aorta has been shown to increase with age,[9] how mitophagy is altered by aging in the cerebral vasculature and its relationship to BBB integrity are unclear.

In this study, we measured mitochondrial function, mitophagy, and inflammatory pathways in the cerebral vessels of young and aged mice to determine if any of these factors correlate with BBB integrity and function.

## METHODS

The data that support the findings of this study are available from the corresponding author upon reasonable request.

### Mice and Diet

Wild-type (WT) young (2–3 months) and aged (18–19 months) male and female C57BL/6 mice were obtained from the National Institute on Aging rodent colony. mtKeima, mitophagy reporter mice on the FVB/NCrl background were generously provided by Dr Finkel.[23] These mice were aged to the indicated ages under specific pathogen-free conditions in the animal facility at the University of Michigan. Tissues from mice were randomly assigned into different treatment groups for in vitro culture. For this study, only aged male mtKeima mice were available. All mice were maintained on a 12-hour light-dark cycle with free access to food (3% calories from fat; LabDiet catalog No. 5001) and water.

## Cerebrovascular Permeability

Cerebrovascular permeability was determined by quantifying Evans Blue extravasation in the brain.[24] Evans Blue (2%) in PBS was injected intravenously. After 30 minutes, the circulation was perfused with 20 mL PBS at a rate of 2 mL/min through the left ventricle of the heart. The right atrium was clipped, and the perfusate was monitored to ensure it ran clear. After perfusion, the brain was harvested, homogenized in 1 mL formamide, and incubated 18 hours at 4°C. Samples were centrifuged at 1000*g* for 30 minutes at 4°C, and the absorbance of the supernatant was analyzed at 610 nm and normalized to brain weight.

## Fluorescence Imaging

For assessment of mean tetramethylrhodamine (ThermoFisher, catalog No. I34361) fluorescence intensity, the left and right middle cerebral arteries (MCAs) were isolated and incubated with PBS+tetramethylrhodamine (100 nmol/L) for 30 minutes at 37°C. The MCAs were washed in PBS twice for 3 minutes before mounting in PBS on glass slides. Imaging commenced immediately following the final wash. Imaging was done using a Nikon A1si confocal microscope with excitation at 488 nm and emission of 560 to 580 nm. Tetramethylrhodamine accumulation in mitochondria is dependent on mitochondrial membrane potential ($\Delta\psi m$). For immunohistochemistry, fixed paraffin-embedded sections of the MCA were deparaffinized and rehydrated. After blocking, sections (6 μm each) were incubated at room temperature for 1 to 2 hours with Parkin (Abcam, catalog No. ab77924; 1:500). After rinsing in PBS, slides were incubated with secondary antibodies for 1 hour at room temperature. Slides were mounted with Prolongold Diamond Antifade mountant (ThermoFisher Scientific, catalog No. P36961). Immunofluorescence images were captured using a Nikon A1si confocal microscope, and colocalization was analyzed using ImageJ. For imaging Parkin, the pixel size is 188.57 nm/pixel at 60× objective. Parkin mean fluorescence intensity was measured within a region of interest that was traced around the α-smooth muscle actin$^+$ layer of cells (ie, the media layer) and averaged to the area of the region of interest. For both tetramethylrhodamine and Parkin imaging, between 3 and 6 representative images for each mouse were collected, and average of the mean fluorescence intensity was reported. Image analysis for mean fluorescence intensity was quantified using ImageJ (NIH, Bethesda, MD). Investigators were blinded when performing analysis.

For assessment of mitophagy index using mtKeima mice, the left and right MCAs were isolated and incubated in medium consisting of 0.5 mmol/L EGTA (Sigma, catalog No. E4378), 3 mmol/L $MgCl_2$ 6 hexahydrate (Sigma, catalog No. M9272), 60 mmol/L lactobionic acid (Sigma, catalog No. 153516), 20 mmol/L taurine (Sigma, catalog No. T0625), 10 mmol/L $KH_2PO_4$ (Sigma, catalog No. P5655), 20 mmol/L HEPES (ThermoFisher Scientific, catalog No. 15630080), 110 mmol/L D-sucrose (Sigma, catalog No. S0389), 1.25 mmol/L ADP (CalBiochem, catalog No. 117105), 2 mmol/L malate (Sigma, catalog No. M1000), 5 mmol/L pyruvate (Sigma, catalog No. P2256), 10 mmol/L glutamate (Sigma, catalog No. G1626), 10 mmol/L succinate (Sigma, catalog No. S2378), and 1 g/L bovine serum albumin at pH 7.1. The MCA was cultured for 2 hours at 37°C with 1 μmol/L rotenone (Sigma, catalog No. R8875), recombinant IL-6 (Peprotech, catalog No. 216-16), or vehicle (PBS or ethanol) for 2 hours at 37°C. Mitotracker green FM (ThermoFisher Scientific, catalog No. M7514) was added during the final 20 minutes of the 2-hour culture period as our microscope does not have the capability to analyze the mtKeima green signal (ie, excitation at 561 nm and detected in the 590–650 nm emission range). Imaging was done using a Nikon A1si confocal microscope. The mtKeima red fluorescent signal was obtained with excitation at 561 nm and detected in the 590- to 650-nm emission range, and the green signal was obtained by excitation at 488 nm and detected within the 500- to 550-nm emission range. Image analysis was done using ImageJ. For mtKeima analysis, mean fluorescence intensity from red 561-nm excitation was normalized to mean green 488-nm excitation fluorescence intensity. Calculating the ratio of red:green fluorescence allows one to quantify the proportion of the total mitochondria that are in the low pH environment of the lysosome.

## Isolation of Cerebral Vessels for Immunoblotting, Mitochondrial DNA Copy Number, and Oxygen Consumption Rate

Cerebral vessels, primarily consisting of arteries, were manually dissected using a dissection microscope similar to what has been previously published.[25,26] Dissected vessels included the circle of Willis, anterior cerebral artery, MCA, interior cerebral arteries, posterior communicating arteries, superior cerebral arteries, basilar artery, and superficial branching arteries on the dorsal cerebral surface, including the rostral and caudal branches of the MCA. Representative immunoblots of isolated vessels are shown in Figure S1.

## Ex Vivo Stimulation

For N-formyl peptide culture, the cerebral vessels from young (2–3 months old) WT mice were dissected,

harvested, and washed in PBS. Cerebral vessels from left and right hemisphere were kept separate from each mouse brain and were randomized for 30-minute culture in PBS with either 10 μmol/L N-formyl peptide (N-Formyl-Nle-Leu-Phe-Nle-Tyr-Lys; Genscript catalog No. RP12959) or vehicle (PBS+1% dimethyl sulfoxide), similar to what was previously done.[15] After 30-minute culture, vessels were washed twice in PBS and immediately flash frozen for immunoblot analysis. For recombinant IL-6 culture, the cerebral vessels from young (2–3 months old) mice were dissected, harvested, and washed in PBS. For recombinant IL-6 culture, cerebral vessels were cultured in DMEM+10% fetal bovine serum with either 0 or 10 ng/mL of recombinant IL-6 (PeproTech, catalog No. 216-16) or vehicle for 2 hours. After 2 hours of IL-6 culture, the tissue was washed 3× with PBS, flash frozen, and used for immunoblot analysis. For anti–IL-6 culture, cerebral vessels were cultured in DMEM+10% fetal bovine serum with either 5 μg/mL anti–IL-6 antibody or IgG control (R&D Systems, catalog No. MAB406, clone MP5-20F3) for 2 hours. After 2-hour culture, tissue was washed 3× with PBS and flash frozen for use immediately for respirometry studies.

## Immunoblotting

The cerebral vasculature from young and aged mice was dissected, harvested, washed, and flash frozen. Tissues were homogenized for 30 seconds in lysis buffer (ThermoFisher Scientific, catalog No. 78510) with 1% protease inhibitor cocktail (Sigma, catalog No. P8340) and 1% phosphatase inhibitor cocktail (Sigma, catalog No. P5726) using tissue homogenizer (PRO Scientific, Oxford, CT). Tissue lysates were electrophoresed on 4% to 12% gradient SDS-polyacrylamide gels and transferred to 0.20 μm polyvinylidene difluoride membranes (ThermoFisher Scientific, catalog No. IB401001). Blotted membranes were blocked in PBS+0.1% Tween-20+5% BSA for 2 hours at room temperature. Membranes were incubated for 1 hour at room temperature with primary antibodies against cytochrome C oxidase IV (1:1000, Abcam, catalog No. ab16056), Parkin (Abcam, catalog No. ab77924; 1:500), Nix (Santa Cruz Biotechnology, catalog No. sc-166332; 1:200), peroxisome proliferator-activated receptor γ coactivator 1-α (Abcam, catalog No. ab54481; 1:1000), cyclin-dependent kinase inhibitor 1 (p21) (Santa Cruz Biotechnology, catalog No. sc-6246; 1:200), STING (Cell Signaling Technology, catalog No. 13647; 1:1000), IL-6 (Cell Signaling Technology, catalog No. 12912; 1:500), formyl peptide receptor 1 (FPR1) (Abcam, catalog No. ab113531; 1:500), Claudin-5 (Abcam, catalog No. ab15106; 1:1000), and β-actin (Abcam, catalog No. ab8226; 1:1000). After washing in PBS+0.1% Tween-20, membranes were incubated in secondary antibodies for 30 minutes (Abcam, catalog No. ab205718 and No. ab205719; 1:5000-1:10 000) and then illuminated with chemiluminescent substrate (ThermoFisher Scientific, catalog No. 34577) using a BioRad ChemiDoc (Hercules, CA). Semiquantitative densitometry was calculated using ImageJ.

## Mitochondrial DNA Copy Number

The cerebral vasculature was harvested, as described above, and flash frozen. DNA was isolated using DNeasy Blood and Tissue Kit (Qiagen, catalog No. 69504). The ratio of mitochondrial DNA copy number/nuclear DNA copy number was determined by real-time polymerase chain reaction (Detroit R&D, catalog No. MCN3), according to manufacturer's instructions using 4 ng of DNA samples. The fold-change was calculated using ΔΔ threshold cycle method and normalized to the young control group.

## Respirometry of Cerebral Vessels

The cerebral vessels were placed in ice-cold respiration medium consisting of 0.5 mmol/L EGTA (Sigma, catalog No. E4378), 3 mmol/L $MgCl_2$ 6 hexahydrate (Sigma, catalog No. M9272), 60 mmol/L lactobionic acid (Sigma, catalog No. 153516), 20 mmol/L taurine (Sigma, catalog No. T0625), 10 mmol/L $KH_2PO_4$ (Sigma, catalog No. P5655), 20 mmol/L HEPES (ThermoFisher Scientific, catalog No. 15630080), 110 mmol/L D-sucrose (Sigma, catalog No. S0389), and 1 g/L BSA at pH 7.1.[27] High-resolution oxygen consumption measurements were conducted in 2 mL of MiR05 using the Oroboros Oxygraph 2k (Oroboros Instruments, Innsbruck, Austria). Polarographic oxygen measurements were acquired at 2-second intervals with the steady-state rate of respiration calculated from a minimum of 30 data points and expressed as pmol $s^{-1}$ per mg wet weight. All respiration measurements were conducted at 37°C in a working range [O2] of ≈200 to 100 μmol/L. Respiration was measured with sequential titrations of: 1.25 mmol/L ADP (CalBiochem, catalog No. 117105), 2 mmol/L malate (Sigma, catalog No. M1000), 5 mmol/L pyruvate (Sigma, catalog No. P2256), 10 mmol/L glutamate (Sigma, catalog No. G1626), 10 mmol/L succinate (Sigma, catalog No. S2378), 0.5 μmol/L carbonyl cyanide m-chlorophenyl hydrazone (Sigma, catalog No. C2759), 0.5 μmol/L rotenone (Sigma, catalog No. R8875), and 2.5 μmol/L antimycin-A (Sigma, catalog No. A8674).

## Statistical Analysis

All results are presented as mean±SEM. Normality was determined using Shapiro-Wilk test. Nonparametric tests were used for data that are not normally distributed. Data with one independent variable (ie, age) that

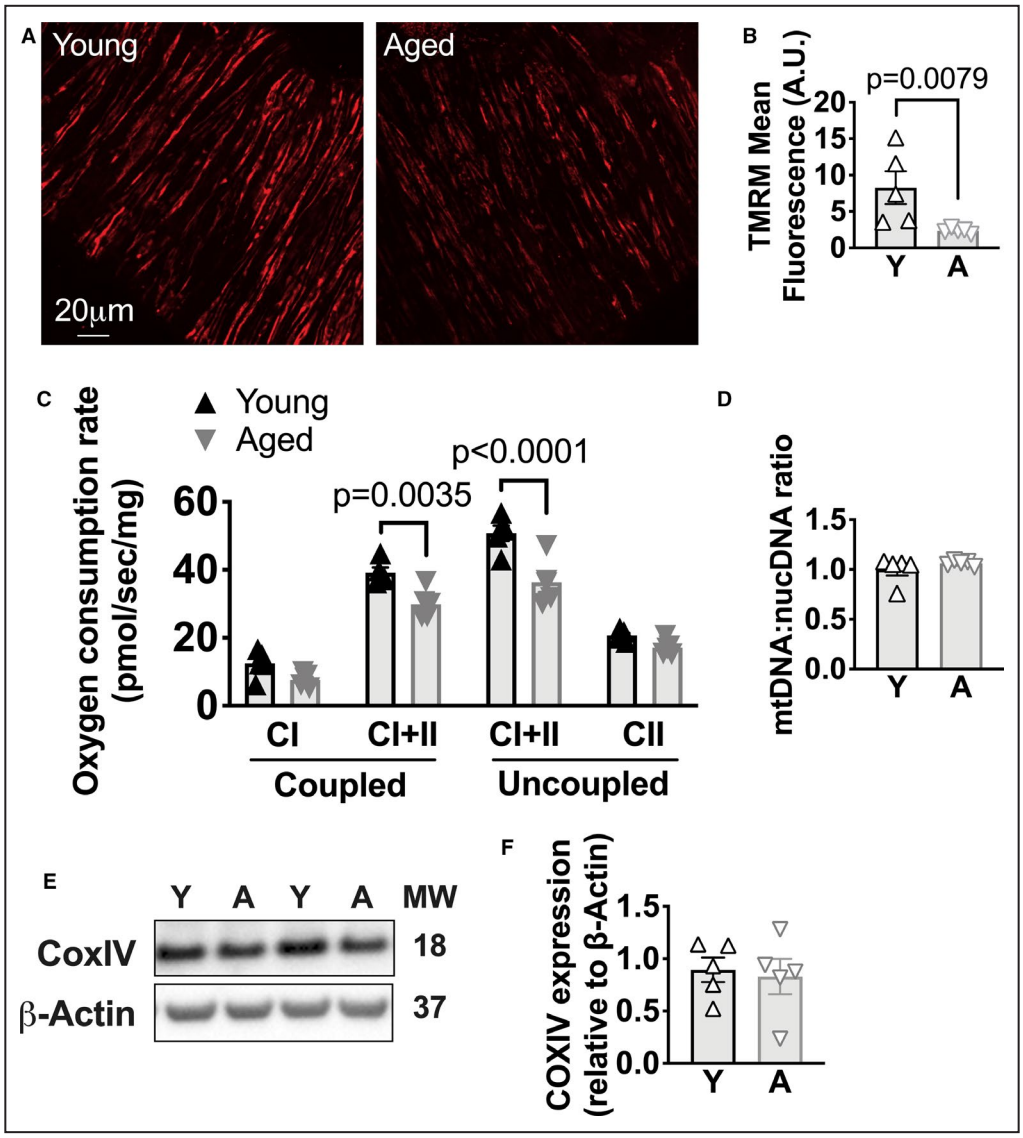


**Figure 1. Aging impairs mitochondrial membrane potential within the cerebral vasculature.** Middle cerebral arteries were obtained from wild-type (WT) female C57LB/6 mice, and mitochondrial membrane potential was measured. **A**, Representative tetramethylrhodamine (TMRM) fluorescence in 3- and 18-month-old female WT mice. **B**, Quantification of mean fluorescence intensity of **A**. **C**, Maximal oxygen consumption rate (OCR) in cerebral vessels with substrates for complex I and I+II coupled oxidative phosphorylation and maximal complex I+II and II uncoupled OCR. **D**, Mitochondrial DNA (mtDNA) copy number/nuclear DNA (nucDNA) copy number ratio. **E**, Cerebral vessel lysates from young and aged mice were immunoblotted against cytochrome C oxidase (Cox) IV and β-actin. **F**, Quantification of immunoblot in **E**. Mann-Whitney *U* test for **B**, **D**, and **F**. Repeated measures 2-way ANOVA with Sidak multiple comparison test for **C**. Each data point represents a biological replicate. N=5 per group. All results are presented as mean±SEM. A indicates aged (18-19 months of age); A.U., arbitrary unit; CI, complex I of the electron transport chain; CII, complex II of the electron transport chain; MW, molecular weight; and Y, young (3–4 months of age).

were generated from 2 groups of mice were analyzed using the Student *t* test or Mann-Whitney *U*-test (non-parametric). When data were generated from the same mouse (ie, cerebral vascular tissue exposed or not to recombinant IL-6), a paired *t* test was used. When >1 independent variable was analyzed (ie, for cerebral vascular oxygen consumption rate experiments), a repeated measures 2-way ANOVA with Sidak multiple comparison test was used. Note, we report specific comparisons between the young and aged groups. For experiments with the aged mtKeima mice, because of limited numbers of mice, the group sizes are not equal. In this case, we used a mixed effect model with repeated measures with the 2-way ANOVA to account

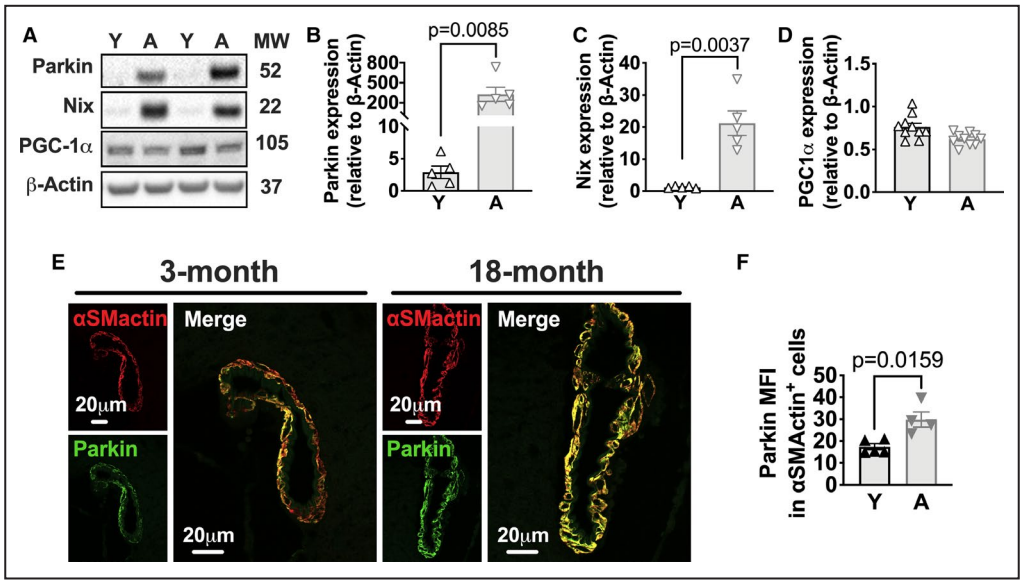


**Figure 2. Aging increases the mitophagy proteins Parkin and Nix within the cerebral vasculature. Middle cerebral arteries (MCAs) were obtained from wild-type female C57LB/6 mice, and the cerebral vasculature was isolated for immunoblot.**

**A**, Cerebral vessel lysates from young (Y; 3-4 months of age) and aged (A; 18–19 months of age) mice were immunoblotted against Parkin, Nix, peroxisome proliferator-activated receptor γ coactivator 1-α (PGC1-α), and β-actin. **B–D**, Quantification of immunoblot in **A**. **E**, Fluorescent staining of α-smooth muscle actin and Parkin in formalin-fixed, paraffin-embedded MCA sections from Y and A mice. **F**, Quantification of Parkin mean fluorescence intensity (MFI) in α-smooth muscle actin$^+$ cell layer. Mann-Whitney *U* test for **B**–**D** and **F**. Each data point represents a biological replicate. N=5 per group for **B** and **C**, N=10 per group for **D,** and N = 4 to 5 for **F**. All results are presented as mean±SEM. αSMactin indicates α-smooth muscle actin; and MW, molecular weight.

for the missing data. Specific statistical tests and *P* values are stated in the figure legends. Two-sided *P* values were used, and values <0.05 were considered significant. Graphpad Prism 8 was used for statistical analysis and figures.

## Study Approval

University of Michigan Institutional Animal Care and Use Committee approved the use of mice for this study.

# RESULTS

## Cerebral Vessels From Aged Mice Exhibit Mitochondrial Dysfunction Compared With Cerebral Vessels From Young Mice

Cerebral vessels were isolated from the brains of healthy young (2–3 months of age) and aged (18–19 months of age) WT female mice, as detailed in the Methods. We first assessed mitochondrial function by measuring basal mitochondrial membrane potential, an established parameter of mitochondrial function,[28] using the fluorescent dye tetramethylrhodamine. We found that the vessels of aged mice exhibited a 3-fold reduction in tetramethylrhodamine signal compared with young mice (Figure 1A and 1B). We next measured oxygen consumption rate (OCR), another established measurement of mitochondrial function,[29] in the cerebral vessels of young and aged mice. Compatible with our findings with tetramethylrhodamine, we found there was an approximate 20% reduction in both coupled and uncoupled complex I and II linked respiration (Figure 1C). The reduction in this signal was not attributable to reduced mitochondrial level, which was measured by mitochondrial DNA:nuclear DNA copy number ratio (Figure 1D), and cytochrome C oxidase IV level, a mitochondrial electron transport chain protein that correlates with mitochondrial mass (Figure 1E and 1F). These data indicate that cerebral vessels exhibit reduced mitochondrial function with aging.

## Mitophagy Proteins Parkin and Nix Are Increased Within the Cerebral Vasculature With Aging

As mitophagy is a key homeostatic process to remove dysfunctional mitochondria,[17] we next assessed levels of the mitophagy proteins, Parkin and Nix. Immunoblot analysis found at least a 10-fold increase in both of these mitophagy proteins in aged

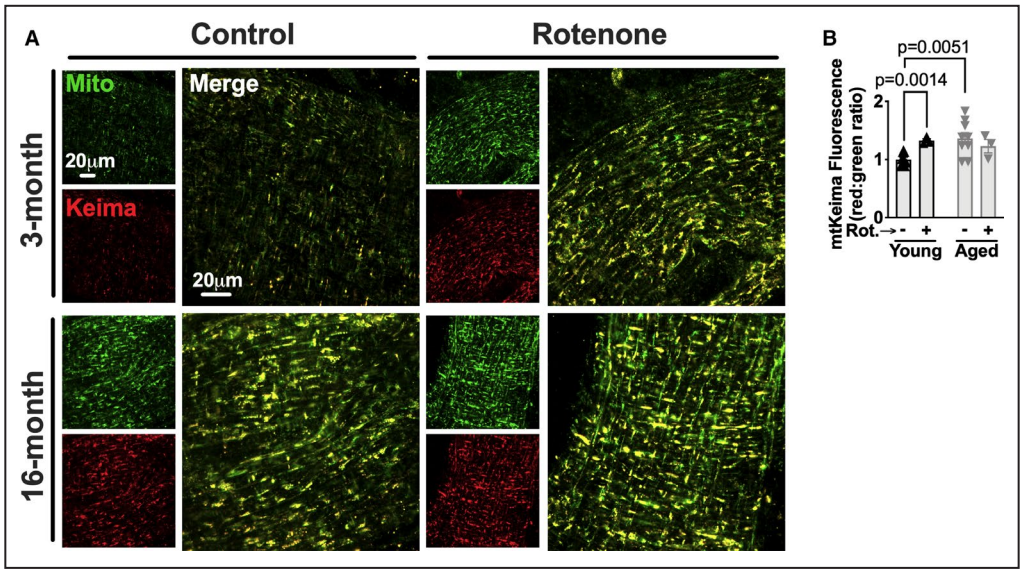


**Figure 3. Mitophagy capacity is impaired in the cerebral vasculature with aging.**
**A** and **B**, Middle cerebral arteries were harvested from young (3–4 months of age) and aged (16–17 months of age) male mtKiema mice (see Methods). The green signal (488-nm excitation) and mtKeima red signal (561-nm excitation) were assessed by fluorescence microscopy (see Methods), and the ratio of 561:488 mean fluorescence intensity (mitophagy index) was calculated in **B**. Scale bars in A=20 μm. Each data point represents a biological replicate. N=9 young and aged mice per group under basal conditions, and N=3 per group with rotenone (Rot.) treatment. All results are presented as mean±SEM. Mixed effect model repeated measures 2-way ANOVA with Sidak post hoc test. Mito indicates mitotracker green FM.

female mice (Figure 2A through 2C), with similar findings in male mice (Figure S2A–S2C), indicating that the upregulation of these proteins occurs regardless of sex. (Note, unless indicated, all the remaining results are with female mice.) We next determined if the increases in these mitophagy proteins with aging correlated with mitochondrial biogenesis. Hence, we measured a key regulator of mitochondrial biogenesis, peroxisome proliferator-activated receptor γ coactivator 1-α (PGC1-α),[30] and found that PGC1-α was similar between aged and young female mice (Figure 2A and 2D) but reduced by 40% in the cerebral vessels of aged male mice (Figure S2A and S2D). Finally, fluorescent microscopic analysis revealed that the age-enhanced increase in Parkin occurred within the smooth muscle cell layer of the cerebral vasculature with aging (Figure 2E and 2F). Hence, these results indicate that 2 mitophagy proteins are increased within the cerebral vasculature with aging, whereas mitochondrial biogenesis may be reduced in aged male mice.

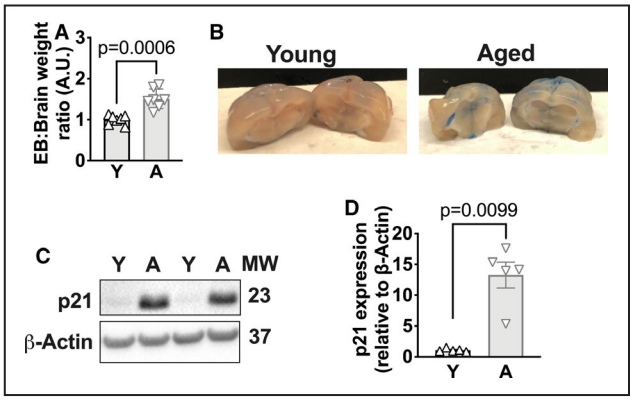


**Figure 4. Aging increases blood-brain barrier leak and associates with an increase in the cyclin-dependent kinase inhibitor 1 (p21) senescent marker.**
Evans Blue (EB) dye was injected into young (Y; 3–4 months of age) and aged (A; 18-19 months of age) female mice intravenously for 30 minutes and washed out with PBS. Brains were extracted, and EB dye extravasation in the parenchyma was quantified. **A**, Quantification of EB dye normalized to brain weight. **B**, Representative images of Y and A brains split coronally to show EB extravasation. **C**, Cerebral vessel lysates from young and aged wild-type C57BL/6 mice were immunoblotted against p21 and β-actin. **D**, Quantification of immunoblot in **C**. Mann-Whitney *U* test for **A** and **D**. Each data point represents a biological replicate. N=7 per group for **A**, and N=5 per group for **D**. All results are presented as mean±SEM. A.U. indicates arbitrary unit; and MW, molecular weight.

## Mitophagy Capacity Is Impaired Within the Cerebral Vasculature With Aging

We next used mitophagy reporter mice (mtKeima) to measure mitophagy within the cerebral vasculature with aging. We recently used these mice to measure mitophagy within the aortas in mice as they age.[9] mtKeima mice express the pH-sensitive and lysosome-resistant protein Keima fused to the mitochondrial targeting sequence from cytochrome C oxidase VIII.[23] As a result, mitochondria in these mice

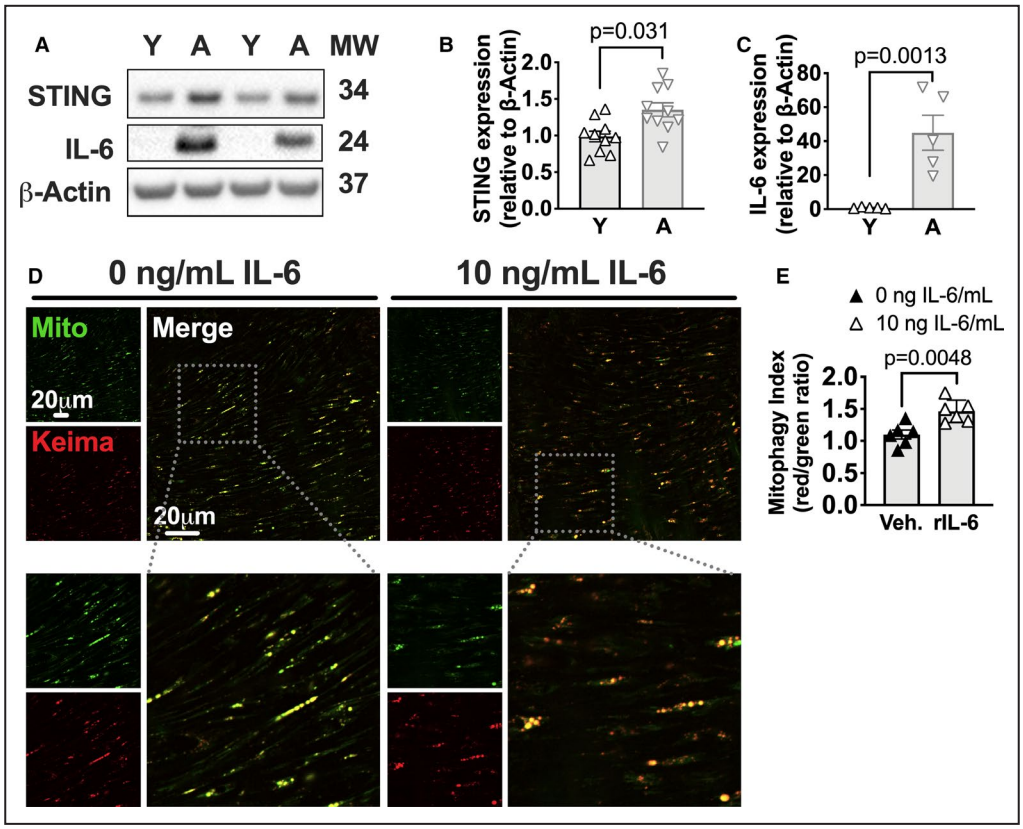


**Figure 5. Aging increases stimulator of interferon genes (STING)–interferon 6 (IL-6) pathway in the cerebral vasculature.**

**A**, Cerebral vessel lysates from young (Y; 3–4 months of age) and aged (A; 18–19 months of age) female wild-type C57BL/6 mice were immunoblotted against STING, IL-6, and β-actin. **B** and **C**, Quantification of immunoblot in **A**. **D**, Middle cerebral arteries were harvested from Y female mtKiema mice (see Methods) and incubated with 0 or 10 ng/mL recombinant IL-6 (rIL-6) for 2 hours. Mitotracker green was added for the final 20 minutes of the incubation following 2 washes with PBS before mounting and imaging. The green signal (488-nm excitation) and mtKeima red signal (561-nm excitation) were assessed by fluorescence microscopy (see Methods), and the ratio of 561:488 mean fluorescence intensity (mitophagy index) is calculated in **E**. Mann-Whitney *U* test for **B** and **C**. Paired *t* test for **E**. Each data point represents a biological replicate. N=10 per group for **A**, N=6 per group for **E**, and N=5 per group for **C**. All results are presented as mean±SEM. Mito indicates mitotracker green FM; MW, molecular weight; and Veh., vehicle.

emit a green fluorescent signal. When mitochondria are shuttled into the lysosomes for degradation, the green signal shifts to a red signal.[23] This allows one to calculate a mitophagy index that reflects mitophagy. We first assessed the mitophagy index in cerebral vessels from young and aged male mtKeima mice under basal conditions. We found that the mitophagy index was increased in the aged vessels compared with the young vessels (Figure 3A and 3B). We next determined the mitophagy index when we activated mitophagy with rotenone, a mitochondrial complex I inhibitor that induces mitophagy.[31] Although the cerebral vessels of young mice exhibited a significant increase in mitophagy index on ex vivo culture with rotenone, cerebral vessels from aged mice failed to do so (Figure 3A and 3B). This indicates the mitophagy capacity within cerebral vessels is impaired with aging.

## Aged Mice Exhibit Increased BBB Leak That Correlates With Increased p21 Protein Expression

We administered Evans Blue dye intravenously into young and aged mice and then assessed the concentration of dye within the brain parenchyma after flushing the systemic circulation to assess leakage of BBB. We found a significant 40% increase in dye concentration in the brains of aged mice compared with young mice (Figure 4A and 4B), indicating a reduction in BBB integrity with aging.

As cellular senescence contributes to BBB integrity,[32] we next measured protein expression of p21, a marker of senescence,[33] in the cerebral vessels of young and aged mice. We found a >10-fold increase in p21 protein levels in aged female cerebral vessels compared with young female cerebral vessels (Figure 4C and 4D).

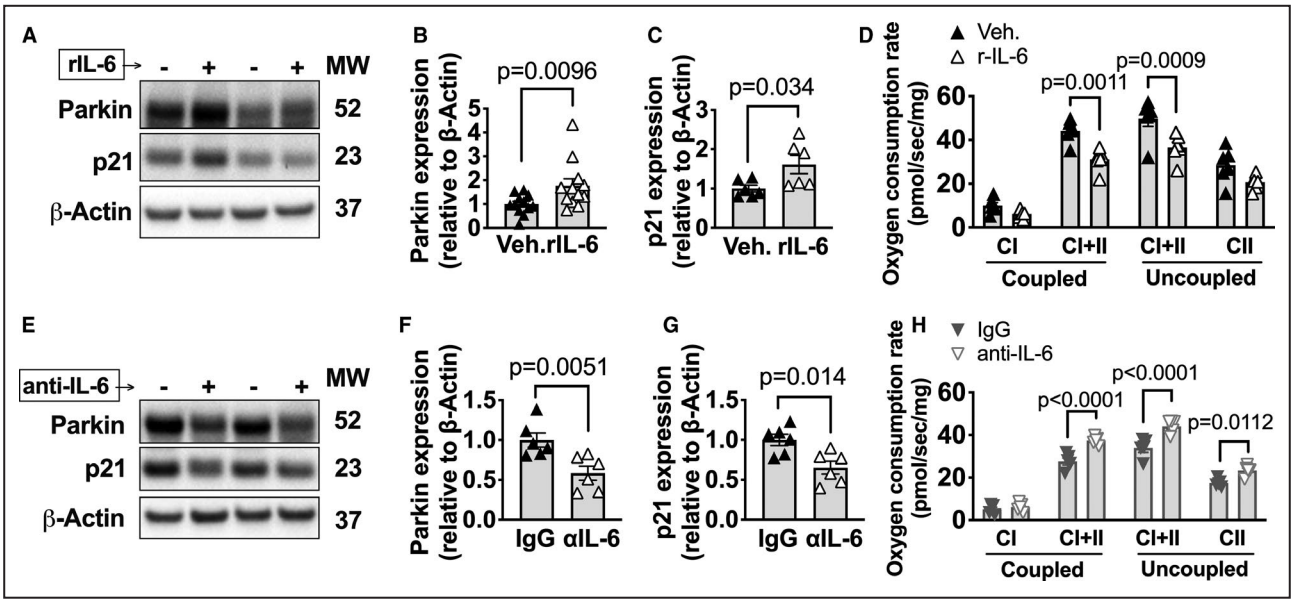


**Figure 6. Interleukin 6 (IL-6) induces Parkin expression and reduces oxygen consumption rate (OCR) in the cerebral vasculature.**

**A**, Cerebral vessel lysates from young (3-4 months of age) wild-type (WT) C57BL/6 mice cultured with exogenous recombinant IL-6 (rIL-6) or vehicle (Veh.) for 2 hours were immunoblotted against Parkin, cyclin-dependent kinase inhibitor 1 (p21), and β-actin. **B** and **C**, Quantification of immunoblot in **A**. **D**, Young cerebral vessels were cultured with either rIL-6 or Veh. for 2 hours. Maximal OCR with substrates for complex I and I+II coupled oxidative phosphorylation (OXPHOS) and maximal complex I+II and II uncoupled OCR were measured. **E**, Cerebral vessel lysates from aged (18–19 months of age) WT C57BL/6 mice cultured with exogenous anti–IL-6 antibody or isotype control for 2 hours were immunoblotted against Parkin, p21, and β-actin. **F** and **G**, Quantification of immunoblot in **E**. **H**, Aged cerebral vessels were cultured with either anti–IL-6 antibody or isotype control for 2 hours. Maximal OCR with substrates for complex I and I+II coupled OXPHOS and maximal complex I+II and II uncoupled OCR was measured. Paired *t* test for **B**, **C**, **F**, and **G**. Repeated measures 2-way ANOVA with Sidak multiple comparison test for **D** and **H**. Each data point represents a biological replicate. N=12 per group for **B**; N=6 per group for **C**, **F**, and **G**; and N=5 per group for **D** and **H**. All results are presented as mean±SEM. CI indicates complex I of the electron transport chain; CII, complex II of the electron transport chain; and MW, molecular weight.

(Similar results were noted in aged male cerebral vessels [Figure S3A and S3B].) Overall, these data indicate that aging increases leak of the BBB and correlates with increased expression of the p21 senescence marker.

## Aged Cerebral Vessels Exhibit Higher Levels of the STING–IL-6 Inflammatory Pathway

Inflammation impairs BBB integrity, which could lead to increased BBB leakage. Given this, we measured levels of inflammatory cytokines and signal adaptors. We found that STING, a signal adaptor that is activated by a variety of intracellular innate recognition pathways,[34] was 40% to 50% upregulated in the vessels of aged mice compared with young mice (Figure 5A and 5B). IL-6 is an inflammatory cytokine that impairs mitophagy[35] and is known to be increased in aged aortas,[9] and was upregulated >5-fold in the cerebral vessels with aging (Figure 5A and 5C). However, we found similar levels of type I interferons, which are typically induced by STING activation, between young or aged vessels (Figure S4A and S4B).The IL-6–STING pathway was also upregulated in the cerebral vessels of aged, male mice (Figure S5).

## IL-6 Induces Mitophagy and Impairs OCR in the Young Cerebral Vasculature, and Blocking IL-6 Induces OCR and Reduces Parkin in the Aged Cerebral Vasculature

We next examined the role of IL-6 on mitophagy in the cerebral vasculature. First, we found that culturing cerebral vessels from young female mtKeima mice with recombinant IL-6 led to a 20% increase in mitophagy index compared with control treated vessels (Figure 5D and 5E). This was associated with a 2-fold upregulation of Parkin in the cerebral vasculature harvested from young WT mice that were cultured with IL-6 (Figure 6A and 6B). Furthermore, we found that IL-6 induced an upregulation of p21 in the cerebral vessels of young WT mice (Figure 6A and 6C). We also found that IL-6 reduced maximal coupled and uncoupled complex I and II OCR in cerebral vessels of young mice (Figure 6D). These results indicate that IL-6 increases mitophagy and impairs mitochondrial function in the cerebral vasculature of young mice.

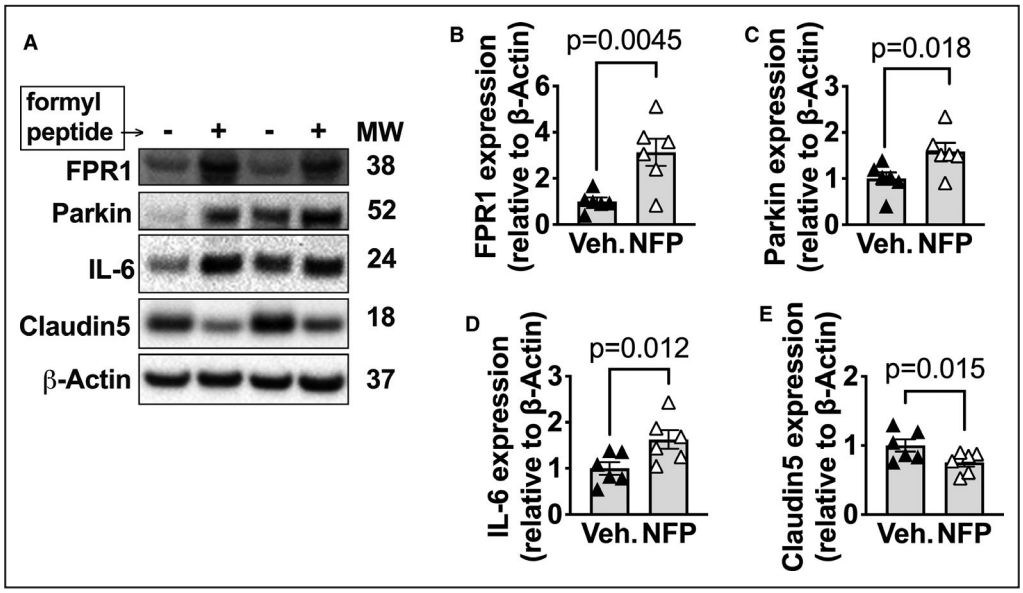


**Figure 7. Formyl peptides upregulate interleukin 6 (IL-6) and Parkin but reduce Claudin-5 expression in young cerebral vessels.**
Cerebral vessels from young mice were isolated and cultured ex vivo with N-formyl peptides (NFPs) or vehicle (Veh.). After culture, cerebral vessels were washed and flash frozen for immunoblot. **A**, Cerebral vessel lysates from young mice cultured with NFP or Veh. were immunoblotted against formyl peptide receptor 1 (FPR1), Parkin, IL-6, Claudin-5, and β-actin. **B**–**E**, Quantification of immunoblot in **A**. Paired *t* test for **B** through **E**. Each data point represents a biological replicate. N=6 per group. All results are presented as mean±SEM. MW indicates molecular weight.

Next, we examined how IL-6 inhibition would alter Parkin expression and OCR in the cerebral vasculature of aged WT mice. (Note, there were insufficient numbers of aged mtKeima mice to perform IL-6 inhibition experiments.) We found that the addition of an IL-6 inhibiting antibody to aged cerebral vessels reduced the expression of Parkin by 30%, reduced p21 by 20% (Figure 6E through 6G), and increased OCR by 30% compared with control-treated aged vessels (Figure 6H). Overall, these data indicate that IL-6 alters mitophagy, increases the p21 senescence marker, and reduces OCR within the aged cerebral vasculature.

## Activating the FPR in the Cerebral Vessels of Young Mice Increases Parkin and IL-6 and Reduces Claudin-5 Levels

Formyl peptides are mitochondrial components that induce inflammation by activating FPR1. We found that cerebral vessels from aged female mice exhibited similar expression of this receptor compared with young counterparts (Figure S6A and S6B). However, aged male vessels exhibited a 2-fold increased expression in FPR1 (Figure S6A and S6B).

To determine if activation of the FPR1 receptor induces inflammation and increases components of mitophagy in cerebral vessels from young (female) mice, we cultured cerebral vessels from young mice with exogenous N-formyl peptides ex vivo. N-formyl peptides induced the upregulation of FPR1 3-fold, Parkin by 50%, and IL-6 by 50% in cerebral vessels from young mice (Figure 7A through 7D). The upregulation of all of these proteins on stimulation with N-formyl peptide concomitantly led to a significant 30% reduction in Claudin-5 protein (Figure 7A through 7E), a tight junction protein that maintains BBB integrity.[36] These data indicate that activation of the FPR1 upregulates Parkin and IL-6 and reduces the expression of the barrier integrity protein, Claudin-5.

# DISCUSSION

How vascular aging impacts mitochondrial function and quality control within the cerebral vasculature is not clear. Our study found that within aged cerebral vessels, mitochondrial function declines, which is coupled to a reduced capacity to remove damaged mitochondria (ie, mitophagy). Furthermore, we have revealed that with aging there is a basal increase in the expression of both the mitophagy protein, Parkin, and the process of mitophagy within the cerebral vasculature. This increased basal mitophagy correlates with a reduced capacity to increase mitophagy on treatment with rotenone. We found that the increase of Parkin occurred within the smooth muscle layer of the cerebral vasculature with aging. However, it is possible that the changes we

have found in our study also occur in other cells of the cerebral vasculature, such as endothelial cells, which should be examined in the future. Aging within the cerebral vasculature also increased the STING–IL-6 pathway, upregulated the p21 senescence marker, and was associated with increased BBB leakage. Treatment of young cerebral vessels with the mtDAMP, N-formyl peptides, upregulated IL-6, and reduced expression of the barrier integrity protein, Claudin-5, which has previously been shown to be reduced with aging.[37]

In our study, IL-6 treatment of young cerebral vessels upregulated the mitophagy protein Parkin, reduced OCR, and increased mitophagy. We complemented these findings by inhibiting IL-6 in aged cerebral vessels and found that blocking IL-6 reduced Parkin and increased OCR. Hence, our study indicates that the age elevation in IL-6, a cytokine that is known to impair mitochondrial function,[35,38] may contribute to altered mitochondrial function and mitophagy within the cerebral vasculature.

Collectively, our study suggests that aging impairs both mitochondrial function and the capacity to remove defective mitochondria within the cerebral vasculature. Combined, there is likely an increased concentration of defective mitochondria within the aged cerebral vasculature. The consequential increase in mtDAMPs activates inflammation to increase IL-6, to further worsen mitophagy, and to reduce BBB integrity. In sum, our study reveals a mechanism as to why the BBB exhibits impaired barrier function with aging and could offer a potential explanation for the subsequent reduced cerebral vascular and neuronal heath that occurs with aging.

During cerebral vascular insults, such as stroke, BBB function is compromised, which could contribute to the pathophysiological features of stroke.[39-41] As the brain is more susceptible to strokes with aging,[42] and aging results in greater neurologic deficit after stroke,[43] our study suggests that the alterations that we have uncovered within the cerebral vasculature with aging without disease could contribute to the age-enhanced risk of stroke. This may be relevant to the 2020 coronavirus disease 2019 pandemic, which is emerging as an age-enhanced disease, in which more severe disease associates with a >10-fold risk of stroke.[44] Our findings are not just relevant to acute insults, such as stroke, but also to chronic neurodegenerative diseases, such as Alzheimer disease, as impaired BBB function may lead to increased deposition or reduced clearance of amyloid-β protein and impaired neuronal health.[45] It will be important in the future to show that enhancing mitochondrial function, mitophagy, or both reduces BBB leak and whether such maneuvers reduce neurological deficits from stroke, or neurodegeneration that occurs with aging.

Our study does not elucidate the temporal alterations between inflammation and impaired mitophagy with aging. Clearly, defective mitophagy and reduced mitochondrial function activate inflammation, likely attributable to mtDAMPs activating intracellular innate immune signaling pathways.[46] As cellular senescence leads to the increased secretion of inflammatory proteins, known as the senescence-associated secretory phenotype,[33] it is also possible that long-term increased secretion of inflammatory proteins by the aged vasculature disrupts vascular bioenergetics, which over time could compromise mitochondrial function. Our study has revealed that the aged cerebral vasculature upregulates IL-6, which has been shown to reduce both mitophagy and mitochondrial function.[9,35] Future studies should investigate if other inflammatory proteins of the senescence-associated secretory phenotype, such as tumor necrosis factor-α or interleukin 1β, are upregulated within the cerebral vasculature with aging. Furthermore, we found that the p21 senescent marker was also upregulated within the aged cerebral vasculature, and that inhibiting IL-6 reduced p21 expression in the cerebral vasculature with aging. This latter result indicates there could be a direct connection with enhanced inflammation and senescence, which should prompt future investigation. Future studies will also be required to determine if inflammation or mitochondrial function is the inciting alteration within the cerebral vasculature with aging. Interestingly, the risk of age-enhanced cardiovascular diseases in humans is reduced in patients who exhibit a loss of function in the *IL6* gene,[47] which should prompt investigation as to whether this is also true for cerebral vascular diseases.

Our study has found that the alterations in the aged cerebral vasculature occur regardless of sex, although there were some alterations that were sex specific. Male aged mice exhibited a reduction in the mitochondrial biogenesis regulatory protein PGC1-α and an increase in FPR1 compared with vessels from young mice, whereas no differences were seen between aged and young female mice. Although our study has not provided an explanation for these findings, estrogens have been suggested as exhibiting a protective role in neurodegenerative diseases.[48] Furthermore, rodent studies have found that female mice may exhibit reduced BBB integrity compared with males.[48] Clearly, future studies are required to characterize the impact of sex in the cerebral vasculature as mice age, and how any sex-specific changes impact cerebral vascular health in general.

In conclusion, our study has revealed that the aged cerebral vasculature exhibits mitochondrial dysfunction coupled to impaired mitophagic capacity. Combined, these alterations increase IL-6 production, which correlates with reduced BBB integrity with aging. These findings inform on how aging

impacts cerebral vascular health and potentially why aging increases cerebral vascular diseases, such as stroke.

## ARTICLE INFORMATION

Received August 11, 2020; accepted October 22, 2020.

### Affiliations

From the Department of Internal Medicine (D.J.T., M.G.B., J.S., S.C.W., D.R.G.)Department of Microbiology and Immunology (D.R.G.) and Institute of Gerontology, University of Michigan, Ann Arbor, MI (D.R.G.).

### Acknowledgments

The authors thank Fran Van den Bergh and Daniel Beard for assistance with respirometry studies. We thank Min Zhang, PhD, of The University of Michigan for her assistance with the statistical analysis of the study. Author contributions: D.J. Tyrrell and D.R. Goldstein conceived, procured funding, and designed research studies. D.J. Tyrrell conducted experiments. D.J. Tyrrell, M.G. Blin, J. Song, S.C. Wood, and D.R. Goldstein analyzed and interpreted data. D.J. Tyrrell and D.R. Goldstein wrote the article. All authors contributed to editing the article.

### Sources of Funding

This work was supported by National Institutes of Health National Research Service Award training grant F32-HL140728 (to D.J. Tyrrell), Multidisciplinary Cardiovascular Research Training Program T32-HL007853 (to D.J. Tyrrell), and R01-HL127687 and R01-AI138347 (both to D.R. Goldstein).

### Disclosures

None.

### Supplementary Material

**Figures S1–S6**

## REFERENCES

1. Zlokovic BV. Neurovascular pathways to neurodegeneration in Alzheimer's disease and other disorders. *Nat Rev Neurosci*. 2011;12:723–738.
2. Foote K, Reinhold J, Yu EPK, Figg NL, Finigan A, Murphy MP, Bennett MR. Restoring mitochondrial DNA copy number preserves mitochondrial function and delays vascular aging in mice. *Aging Cell*. 2018;17:e12773.
3. LaRocca TJ, Hearon CM Jr, Henson GD, Seals DR. Mitochondrial quality control and age-associated arterial stiffening. *Exp Gerontol*. 2014;58:78–82.
4. Ungvari Z, Tarantini S, Donato AJ, Galvan V, Csiszar A. Mechanisms of vascular aging. *Circ Res*. 2018;123:849–867.
5. Ungvari Z, Bailey-Downs L, Sosnowska D, Gautam T, Koncz P, Losonczy G, Ballabh P, de Cabo R, Sonntag WE, Csiszar A. Vascular oxidative stress in aging: a homeostatic failure due to dysregulation of NRF2-mediated antioxidant response. *Am J Physiol-Heart Circ Phys*. 2011;301:H363–H372.
6. Osonoi Y, Mita T, Azuma K, Nakajima K, Masuyama A, Goto H, Nishida Y, Miyatsuka T, Fujitani Y, Koike M, et al. Defective autophagy in vascular smooth muscle cells enhances cell death and atherosclerosis. *Autophagy*. 2018;14:1991–2006.
7. Valcarcel-Ares MN, Gautam T, Warrington JP, Bailey-Downs L, Sosnowska D, de Cabo R, Losonczy G, Sonntag WE, Ungvari Z, Csiszar A. Disruption of Nrf2 signaling impairs angiogenic capacity of endothelial cells: implications for microvascular aging. *J Gerontol A Biol Sci Med Sci*. 2012;67:821–829.
8. Toth P, Tarantini S, Csiszar A, Ungvari Z. Functional vascular contributions to cognitive impairment and dementia: mechanisms and consequences of cerebral autoregulatory dysfunction, endothelial impairment, and neurovascular uncoupling in aging. *Am J Physiol Heart Circ Physiol*. 2017;312:H1–H20.
9. Tyrrell DJ, Blin M, Song J, Wood S, Zhang M, Beard DA, Goldstein DR. Age-associated mitochondrial dysfunction accelerates atherogenesis. *Circ Res*. 2020;126:298–314.
10. Yu EPK, Reinhold J, Yu H, Starks L, Uryga AK, Foote K, Finigan A, Figg N, Pung YF, et al. Mitochondrial respiration is reduced in atherosclerosis, promoting necrotic core formation and reducing relative fibrous cap thickness. *Arterioscler Thromb Vasc Biol*. 2017;37:2322–2332.
11. Wang J, Uryga AK, Reinhold J, Figg N, Baker L, Finigan A, Gray K, Kumar S, Clarke M, Bennett M. Vascular smooth muscle cell senescence promotes atherosclerosis and features of plaque vulnerability. *Circulation*. 2015;132:1909–1919.
12. Zhang JZ, Liu Z, Liu J, Ren JX, Sun TS. Mitochondrial DNA induces inflammation and increases TLR9/NF-kappaB expression in lung tissue. *Int J Mol Med*. 2014;33:817–824.
13. West AP, Khoury-Hanold W, Staron M, Tal MC, Pineda CM, Lang SM, Bestwick M, Duguay BA, Raimundo N, MacDuff DA, et al. Mitochondrial DNA stress primes the antiviral innate immune response. *Nature*. 2015;520:553–557.
14. West AP, Shadel GS, Ghosh S. Mitochondria in innate immune responses. *Nat Rev Immunol*. 2011;11:389–402.
15. Wenceslau CF, McCarthy CG, Szasz T, Goulopoulou S, Webb RC. Mitochondrial N-formyl peptides induce cardiovascular collapse and sepsis-like syndrome. *Am J Physiol Heart Circ Physiol*. 2015;308:H768–H777.
16. Marques F, Sousa JC, Sousa N, Palha JA. Blood-brain-barriers in aging and in Alzheimer's disease. *Mol Neurodegener*. 2013;8:38.
17. Youle RJ, Narendra DP. Mechanisms of mitophagy. *Nat Rev Mol Cell Biol*. 2011;12:9–14.
18. Cornelissen T, Vilain S, Vints K, Gounko N, Verstreken P, Vandenberghe W. Deficiency of parkin and PINK1 impairs age-dependent mitophagy in Drosophila. *eLife*. 2018;7:e35878. http://dx.doi.org/10.7554/elife.35878.
19. Deas E, Plun-Favreau H, Wood NW. PINK1 function in health and disease. *EMBO Mol Med*. 2009;1:152–165.
20. Gladkova C, Maslen SL, Skehel JM, Komander D. Mechanism of parkin activation by PINK1. *Nature*. 2018;559: 410–414. http://dx.doi.org/10.1038/s41586-018-0224-x.
21. Chan NC, Salazar AM, Pham AH, Sweredoski MJ, Kolawa NJ, Graham RL, Hess S, Chan DC. Broad activation of the ubiquitin-proteasome system by Parkin is critical for mitophagy. *Hum Mol Genet*. 2011;20:1726–1737.
22. Klionsky DJ, Abdelmohsen K, Abe A, Abedin MJ, Abeliovich H, Arozena AA, Adachi H, Adams CM, Adams PD, Adeli K, et al. Guidelines for the use and interpretation of assays for monitoring autophagy. *Autophagy*. 2016;12:1–222.
23. Sun N, Yun J, Liu J, Malide D, Liu C, Rovira Ilsa I, Holmström Kira M, Fergusson Maria M, Yoo Young H, Combs Christian A, et al. Measuring in vivo mitophagy. *Mol Cell*. 2015;60:685–696.
24. Goldim MPS, Della Giustina A, Petronilho F. Using evans blue dye to determine blood-brain barrier integrity in rodents. *Curr Protoc Immunol*. 2019;126:e83.
25. Hur JC, Blaise R, Limon I. Protocol for isolating the mouse circle of willis. *J Vis Exp*. 2016;116:e54352. http://dx.doi.org/10.3791/54352.
26. Bowyer JF, Thomas M, Patterson TA, George NI, Runnells JA, Levi MS. A visual description of the dissection of the cerebral surface vasculature and associated meninges and the choroid plexus from rat brain. *J Vis Exp*. 2012;69:e4285. http://dx.doi.org/10.3791/4285.
27. Gnaiger E, Kuznetsov AV, Schneeberger S, Seiler R, Brandacher G, Steurer W, Margreiter R. Mitochondria in the cold. In: Heldmaier G, Klingenspor M, eds. *Life in the Cold*. Berlin, Heidelberg: Springer; 2000:431–442. https://doi.org/10.1007/978-3-662-04162-8_45.
28. Scaduto RC Jr, Grotyohann LW. Measurement of mitochondrial membrane potential using fluorescent rhodamine derivatives. *Biophys J*. 1999;76:469–477.
29. Perry CG, Kane DA, Lanza IR, Neufer PD. Methods for assessing mitochondrial function in diabetes. *Diabetes*. 2013;62:1041–1053.
30. Liang H, Ward WF. PGC-1α: a key regulator of energy metabolism. *Adv Physiol Educ*. 2006;30:145–151.
31. Heinz S, Freyberger A, Lawrenz B, Schladt L, Schmuck G, Ellinger-Ziegelbauer H. Mechanistic investigations of the mitochondrial complex I inhibitor rotenone in the context of pharmacological and safety evaluation. *Sci Rep*. 2017;7:45465.
32. Yamazaki Y, Baker DJ, Tachibana M, Liu C-C, Deursen JMV, Brott TG, Bu G, Kanekiyo T. Vascular cell senescence contributes to blood-brain barrier breakdown. *Stroke*. 2016;47:1068–1077.
33. Tchkonia T, Zhu Y, van Deursen J, Campisi J, Kirkland JL. Cellular senescence and the senescent secretory phenotype: therapeutic opportunities. *J Clin Invest*. 2013;123:966–972.

34. Sliter DA, Martinez J, Hao L, Chen X, Sun N, Fischer TD, Burman JL, Li Y, Zhang Z, Narendra DP, et al. Parkin and PINK1 mitigate STING-induced inflammation. *Nature*. 2018;561:258–262.
35. Marasco MR, Conteh AM, Reissaus CA, Cupit JE, Appleman EM, Mirmira RG, Linnemann AK. Interleukin-6 reduces β-cell oxidative stress by linking autophagy with the antioxidant response. *Diabetes*. 2018;67:1576–1588.
36. Greene C, Hanley N, Campbell M. Claudin-5: gatekeeper of neurological function. *Fluids Barriers CNS*. 2019;16:3.
37. Stamatovic SM, Martinez-Revollar G, Hu A, Choi J, Keep RF, Andjelkovic AV. Decline in Sirtuin-1 expression and activity plays a critical role in blood-brain barrier permeability in aging. *Neurobiol Dis*. 2019;126:105–116.
38. Ji C, Chen X, Gao C, Jiao L, Wang J, Xu G, Fu H, Guo X, Zhao Y. IL-6 induces lipolysis and mitochondrial dysfunction, but does not affect insulin-mediated glucose transport in 3T3-L1 adipocytes. *J Bioenerg Biomembr*. 2011;43:367–375.
39. Doyle KP, Quach LN, Sole M, Axtell RC, Nguyen TV, Soler-Llavina GJ, Jurado S, Han J, Steinman L, Longo FM, et al. B-lymphocyte-mediated delayed cognitive impairment following stroke. *J Neurosci*. 2015;35:2133–2145.
40. Truong DT, Venna VR, McCullough LD, Fitch RH. Deficits in auditory, cognitive, and motor processing following reversible middle cerebral artery occlusion in mice. *Exp Neurol*. 2012;238:114–121.
41. Hattori K, Lee H, Hurn PD, Crain BJ, Traystman RJ, DeVries AC. Cognitive deficits after focal cerebral ischemia in mice. *Stroke*. 2000;31:1939–1944.
42. Manolio TA, Kronmal RA, Burke GL, O'Leary DH, Price TR. Short-term predictors of incident stroke in older adults: *the Cardiovascular Health Study. Stroke*. 1996;27:1479–1486.
43. Ritzel RM, Lai YJ, Crapser JD, Patel AR, Schrecengost A, Grenier JM, Mancini NS, Patrizz A, Jellison ER, Morales-Scheihing D, et al. Aging alters the immunological response to ischemic stroke. *Acta Neuropathol*. 2018;136:89–110.
44. Wang D, Hu B, Hu C, Zhu F, Liu X, Zhang J, Wang B, Xiang H, Cheng Z, Xiong Y, et al. Clinical characteristics of 138 hospitalized patients with 2019 novel coronavirus-infected pneumonia in Wuhan, *China. JAMA*. 2020;323:1061–1069.
45. Chan-Ling T, Hughes S, Baxter L, Rosinova E, McGregor I, Morcos Y, van Nieuwenhuyzen P, Hu P. Inflammation and breakdown of the blood-retinal barrier during "physiological aging" in the rat retina: a model for CNS aging. *Microcirculation*. 2007;14:63–76.
46. Wallings RL, Herrick MK, Tansey MG. Linking mitochondria to the immune response. *Elife*. 2020;9:e56214.
47. Bick AG, Pirruccello JP, Griffin GK, Gupta N, Gabriel S, Saleheen D, Libby P, Kathiresan S, Natarajan P. Genetic interleukin 6 signaling deficiency attenuates cardiovascular risk in clonal hematopoiesis. *Circulation*. 2020;141:124–131.
48. Sohrabji F. Guarding the blood–brain barrier: a role for estrogen in the etiology of neurodegenerative disease. *Gene Expr*. 2006;13:311–319. http://dx.doi.org/10.3727/000000006781510723.

# Supplemental Material

**Figure S1. Isolation of cerebral vessels.**

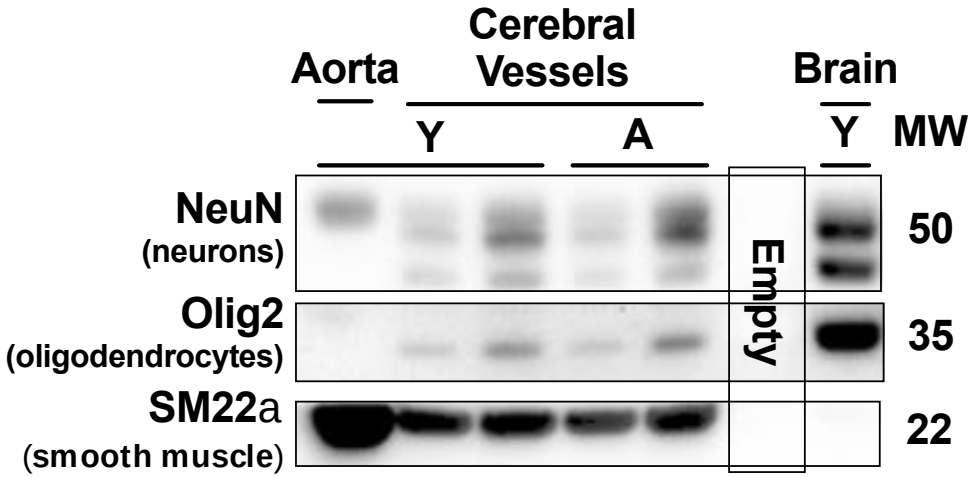


Representative immunoblot of ascending and descending thoracic aorta, brain, and cerebral vessels were dissected from mice (see Methods) and flash-frozen for immunoblot. Protein concentration was determined by BCA assay and 20μg of each lysate was electrophoresed and immunoblotted against a neuronal marker (NeuN), oligodendrocyte marker (Olig2), and smooth-muscle cell marker (SM22α). Each lane represents an individual biological replicate. Results were similar in young and aged brains. A = aged (18-19 months of age); and Y = young (3-4 months of age).

**Figure S2. Aging increase Parkin and Nix in the cerebral vessels of aged male mice.**

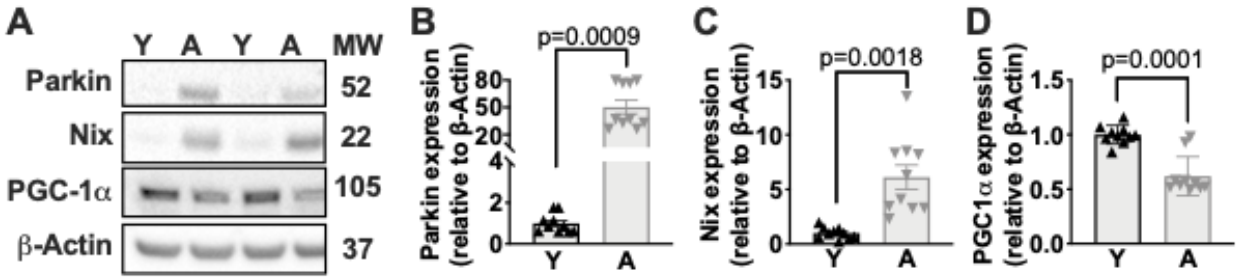


**A**: Cerebral vessel lysates from young and aged male WT C57BL/6 mice were immunoblotted against Parkin, Nix, PGC1-α, and β-actin. **B**-**D**: Quantification of immunoblot in **A**. Mann-Whitney *U* test for **A-D**. Each data point represents a biological replicate. N=10 mice per group. All results are presented as mean ±SEM. A = aged (18-19 months of age); and Y = young (3-4 months of age).

**Figure S3. Aging increases p21 in the cerebral vessels of aged male mice.**

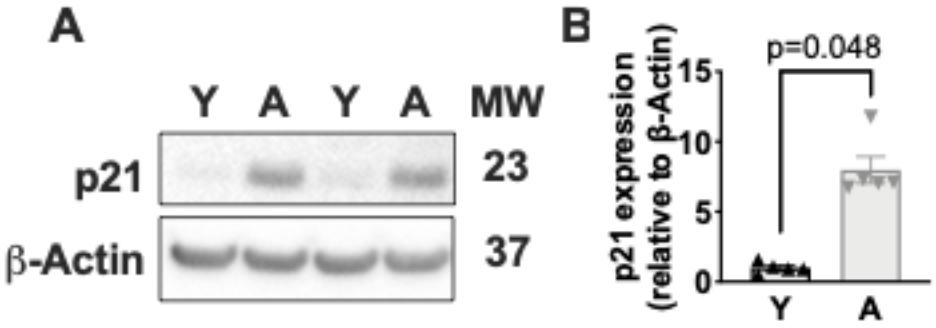


**A**, Cerebral vessel lysates from young and aged WT male C57BL/6 mice were immunoblotted against p21 and β-actin. **B**: Quantification of immunoblot in **A** and **B**. Mann-Whitney *U* test for **A**. N=5 mice per group. Each data point represents a biological replicate. All results are presented as mean ±SEM. A = aged (18-19 months of age); and Y = young (3-4 months of age).

**Figure S4. IFNβ expression in the cerebral vessels of mice.**

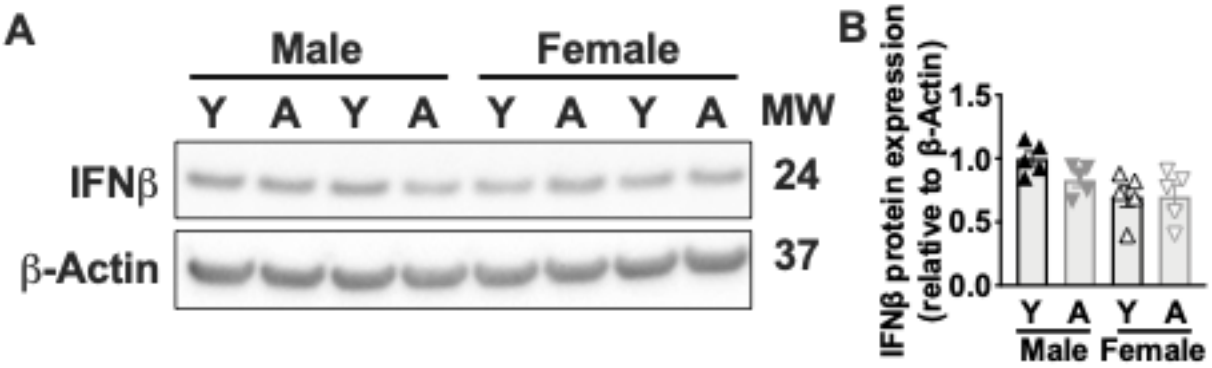


**A**, Cerebral vessel lysates from young and aged WT C57BL/6 mice were immunoblotted against IFN β and β-actin. **B**: Quantification of immunoblot in **A**. Mann-Whitney *U* test for **A** and **B**. Each data point represents a biological replicate. N=5 mice per group. All results are presented as mean ±SEM. A = aged (18-19 months of age); and Y = young (3-4 months of age).

**Figure S5. Aging increases STING-IL-6 in the cerebral vessels of aged male mice.**

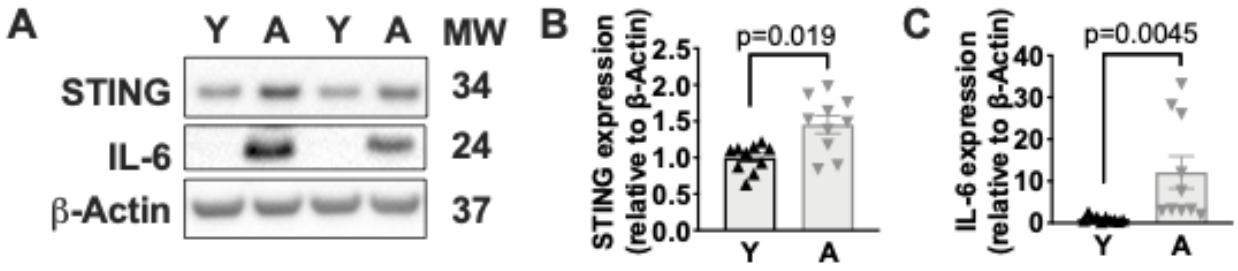


**A**: Cerebral vessel lysates from young and aged WT C57BL/6 male mice were immunoblotted against STING, IL-6, and β-actin. **B**: Quantification of immunoblot in **A**. Mann-Whitney *U* test for **A**-**C**. Each data point represents a biological replicate. N=10 mice per group. All results are presented as mean ±SEM. A = aged (18-19 months of age); and Y = young (3-4 months of age).

**Figure S6. Aging increase FPR1 in the cerebral vessels of aged mice.**

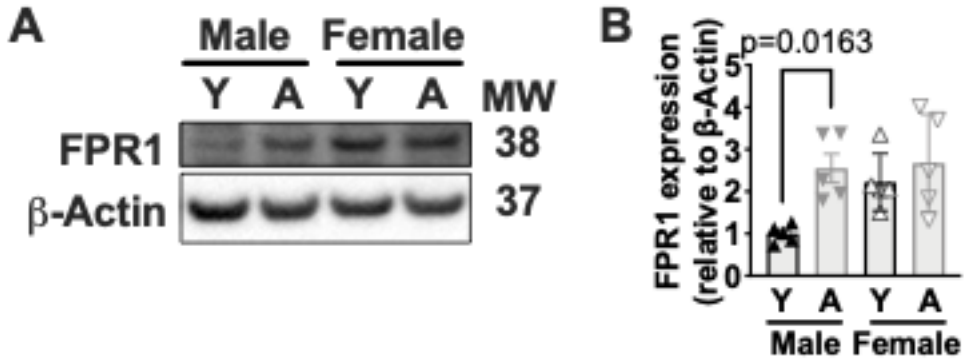


**A**: Cerebral vessel lysates from young and aged WT C57BL/6 mice were immunoblotted against FPR1 and β-actin. **B**: Quantification of immunoblot in **A**. Mann-Whitney *U* test for **A** and **B**. Each data point represents a biological replicate. N=5 mice per group. All results are presented as mean ±SEM. A = aged (18-19 months of age); and Y = young (3-4 months of age).